

Supporting Information

Computational investigation of UiO-66 confinement effect on copper clusters: initial hydrogenation of CO₂

Zechen Ye,^a Wenxuan Xie,^b Hongyan Chen^{c*}, Sibudjing Kawi,^{a*}

^a *Department of Chemical and Biomolecular Engineering, National University of Singapore, 117576, Singapore*

^b *Waste Water Treatment Plant, Yuancheng district, Heyuan 517099, China*

^c *School of Chemistry and Materials Engineering, Huizhou University, Huizhou 516007, China*

*Corresponding author: chenhy@hzu.edu.cn, chekawis@nus.edu.sg

Table of Contents

S1. CO ₂ hydrogenation.....	2
S2. Selection of active sites.....	10
S3. Validations of input parameter.....	13
S4. References.....	14

S1. CO₂ hydrogenation

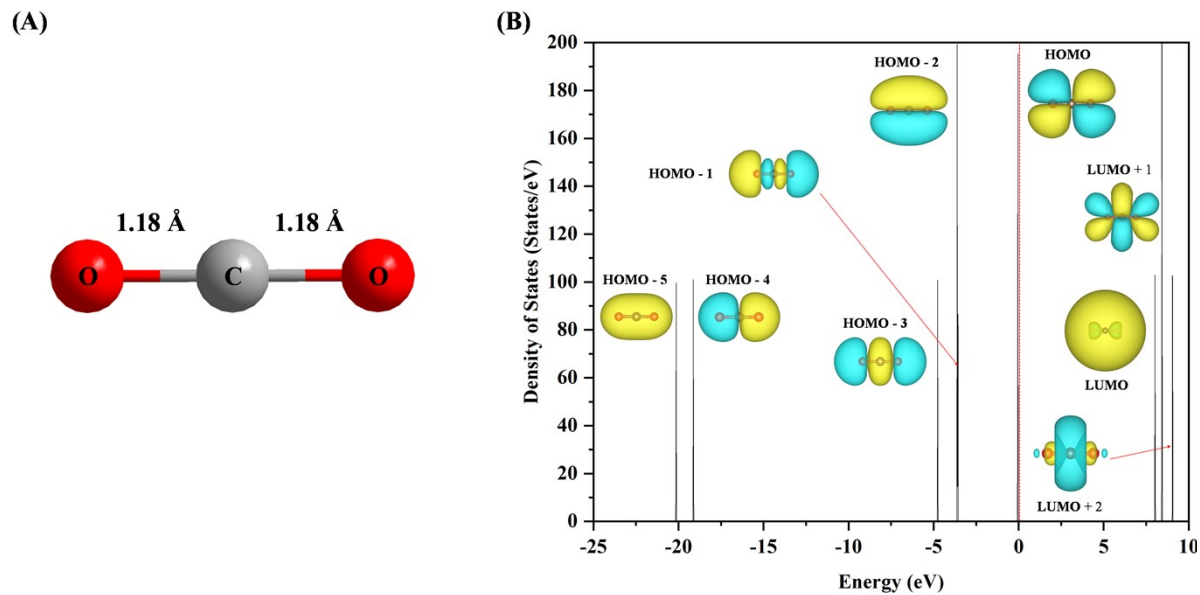


Figure S1. The (A) optimized structure with key bond distance in Å and (B) density of states (DOS) of CO₂ in gas phase.

Table S1. Adsorption energy of H* on catalyst surface ΔE_H obtained using equation: $\Delta E_H = E - E_{\text{catalyst}} - E_H$, where E , E_{catalyst} and E_H are electronic energies of adsorption system, catalyst and gas-phase H atom, as well as d-band center (ε_d) of Cu₈, Cu₁₆, Cu₈@UiO-66 and Cu₁₆@UiO-66.

Catalyst	Cu ₈	Cu ₁₆	Cu ₈ @UiO-66	Cu ₁₆ @UiO-66
ΔE_H (kcal mol ⁻¹)	-47.01	-57.52	-61.42	-63.70
ε_d (eV)	-1.26	-1.88	-1.86	-1.99

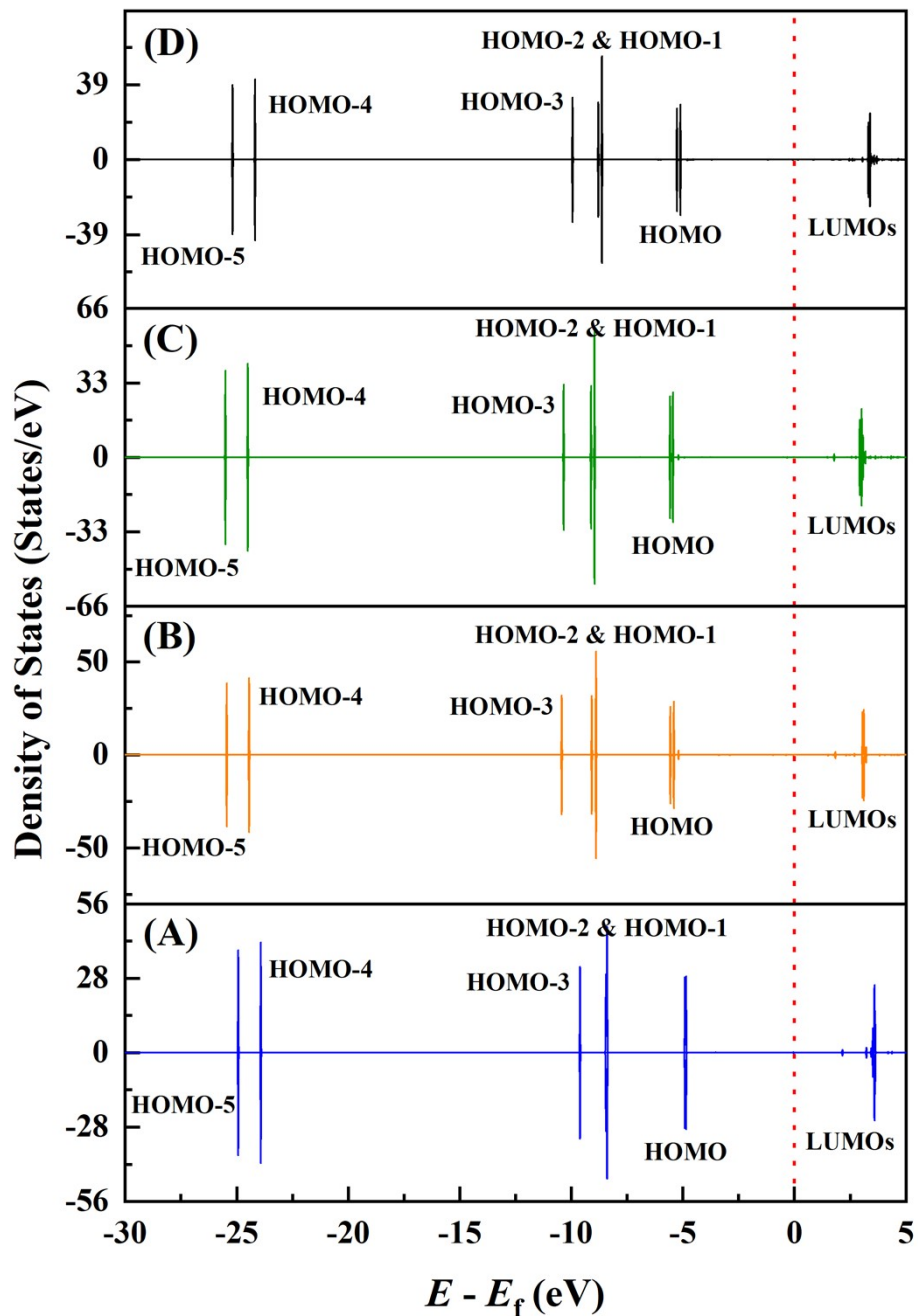


Figure S2. The density of states (DOS) of CO₂ on non-confined (A) Cu₄, (B) Cu₈, (C) Cu₁₆ and (D) Cu₃₂.

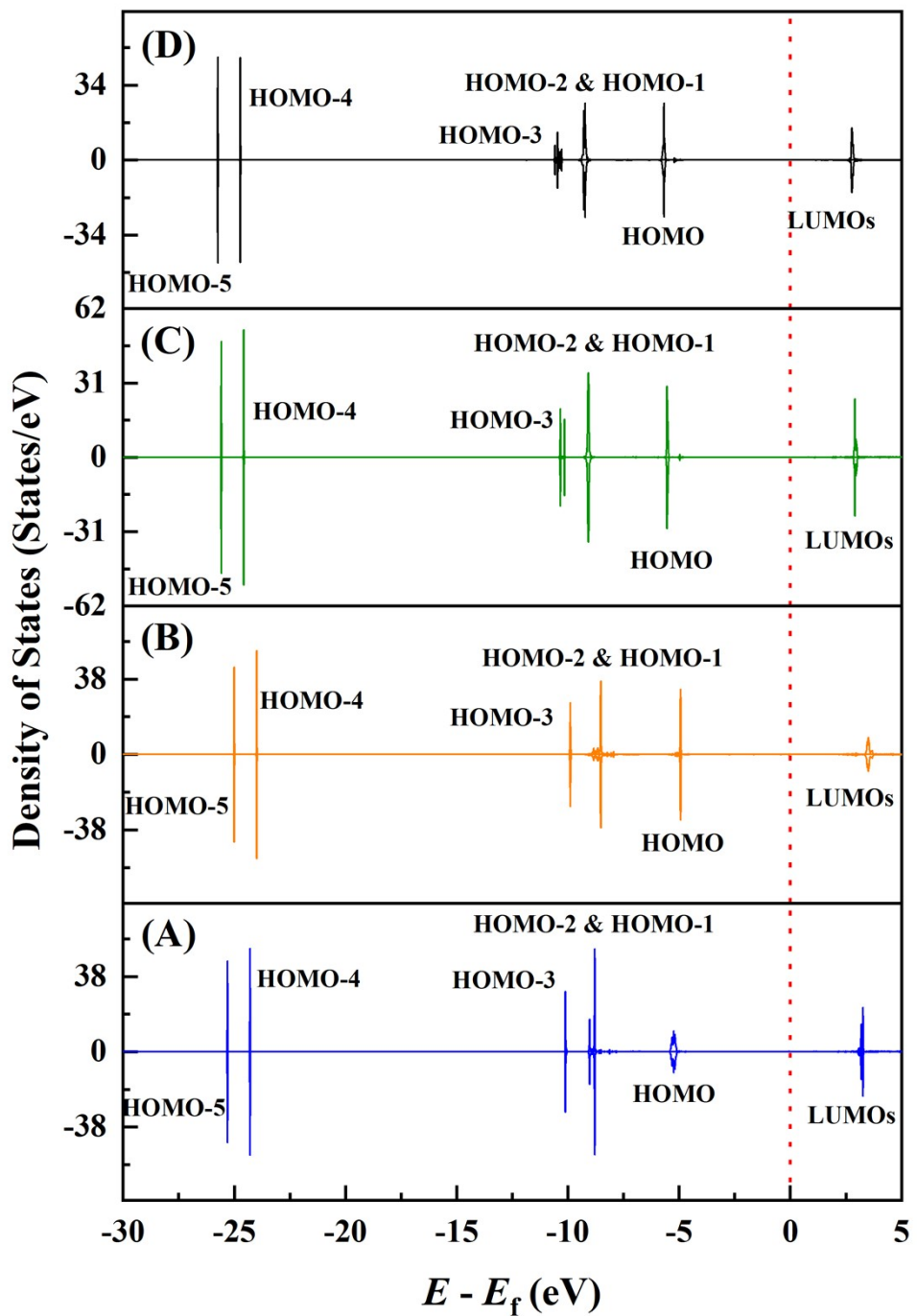


Figure S3. The density of states (DOS) of CO_2 on UiO-66-confined (A) Cu_4 , (B) Cu_8 , (C) Cu_{16} and (D) Cu_{32} .

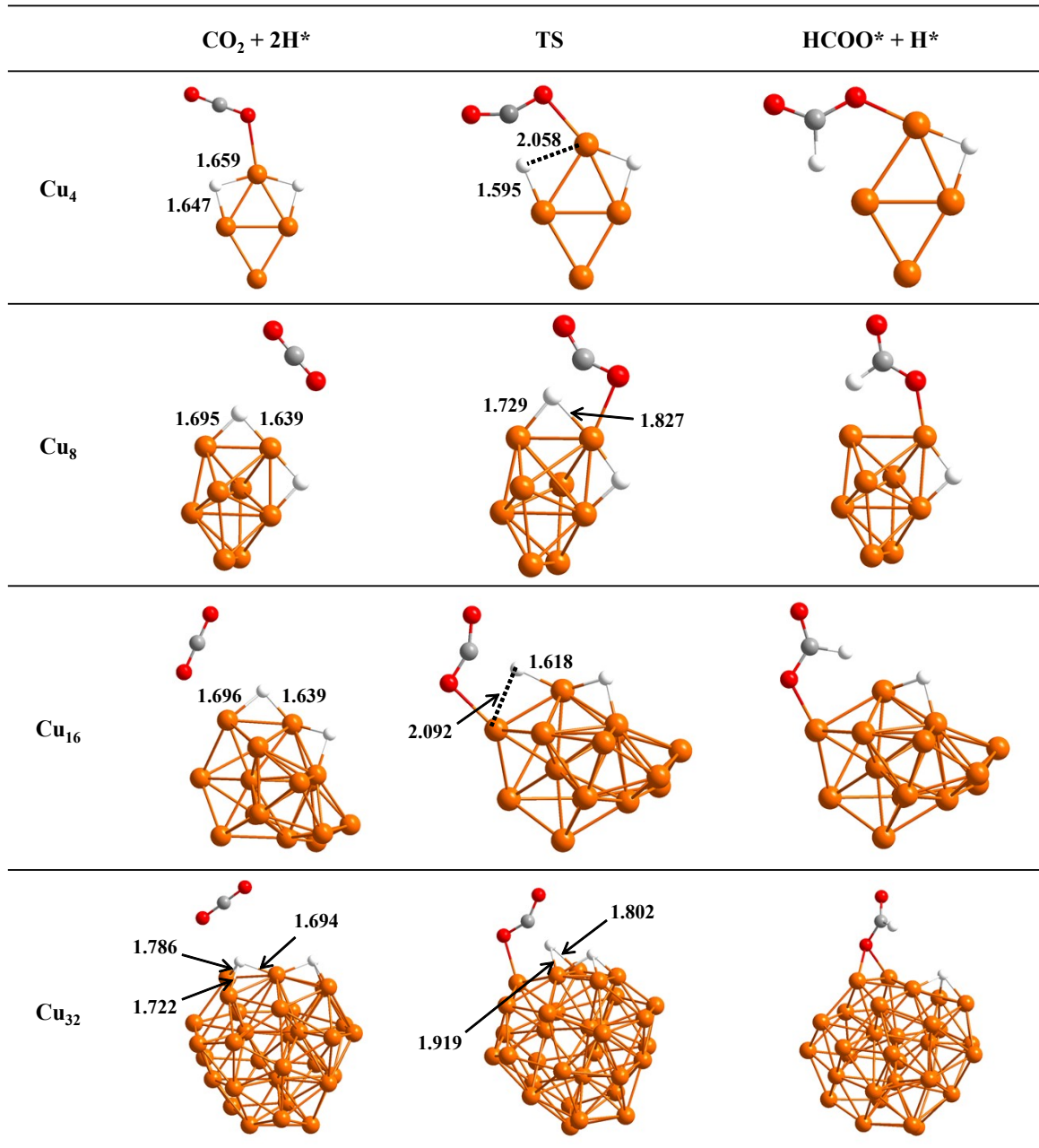


Figure S4. The optimized structures of CO_2 hydrogenation on non-confined Cu_n ($n = 4, 8, 16, 32$) with key bond distance (\AA), where H C, O and Cu are in white, grey, red and orange, respectively.

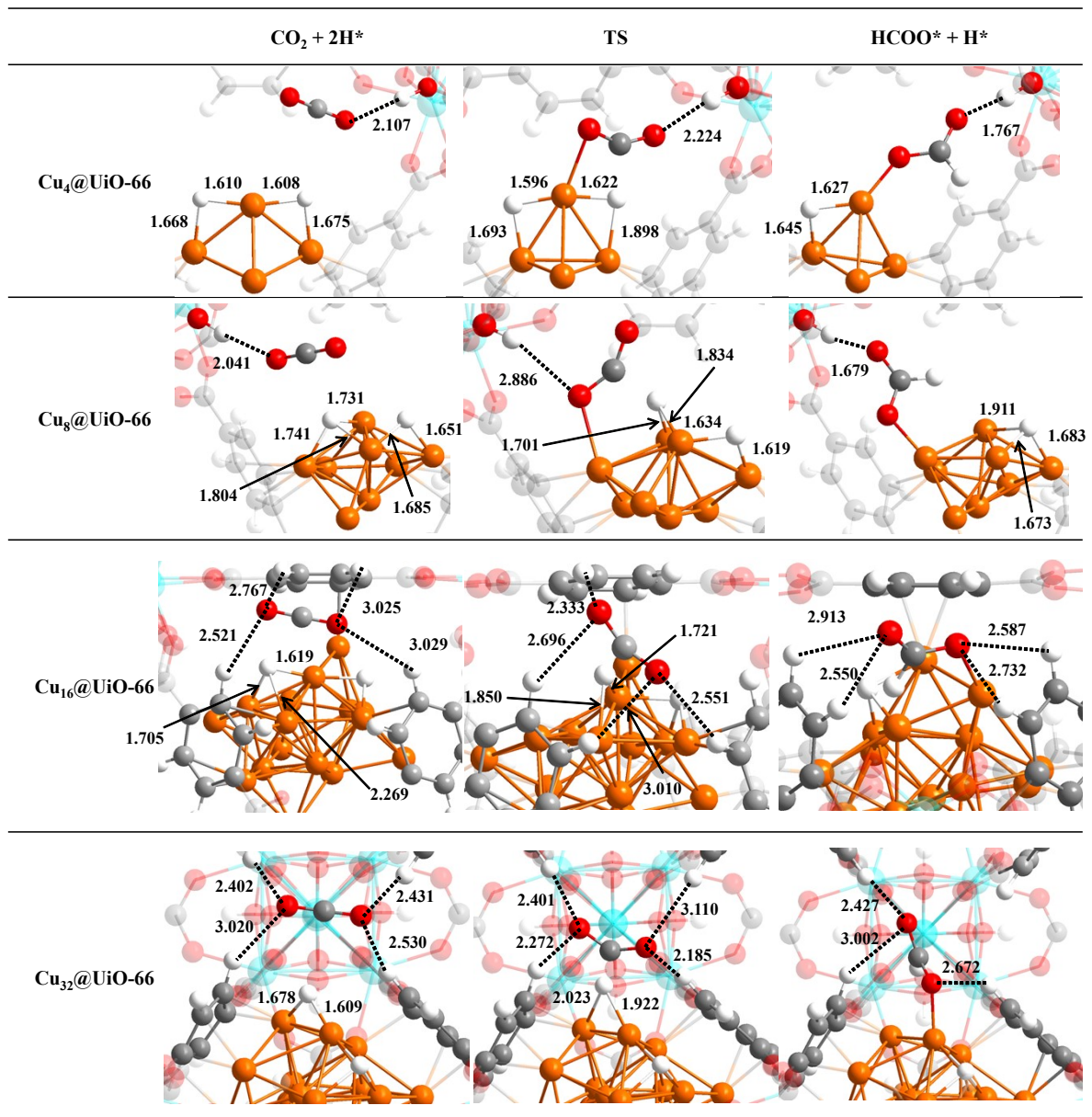


Figure S5. The optimized structures of CO_2 hydrogenation on UiO-66 -confined Cu_n ($n = 4, 8, 16, 32$) with key bond distance (\AA), where H, C, O, Zr and Cu are in white, grey, red, turquoise and orange, respectively.

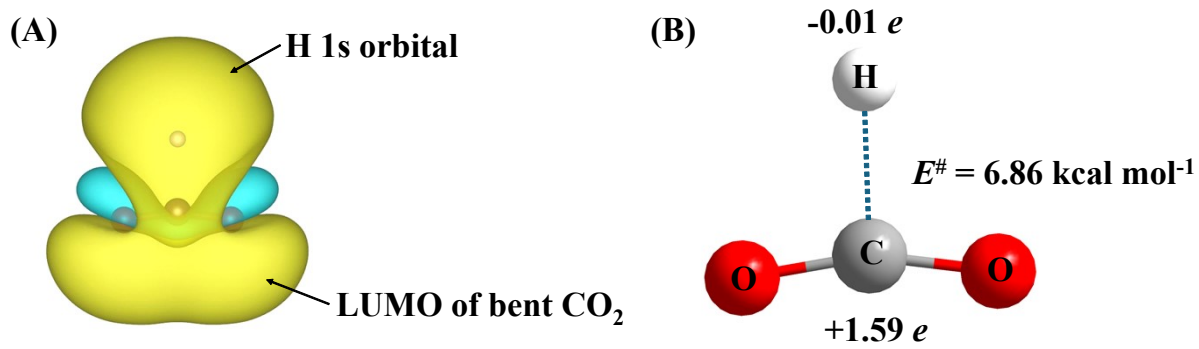


Figure S6. (A) Overlap between H 1s orbital and lowest unoccupied molecular orbital (LUMO) of bent CO_2 ; (B) Optimized structure of CO_2 hydrogenation to HCOO in gas phase, where charge state of C and H atoms are labeled, $E^\#$ is the activation barrier in kcal mol^{-1}

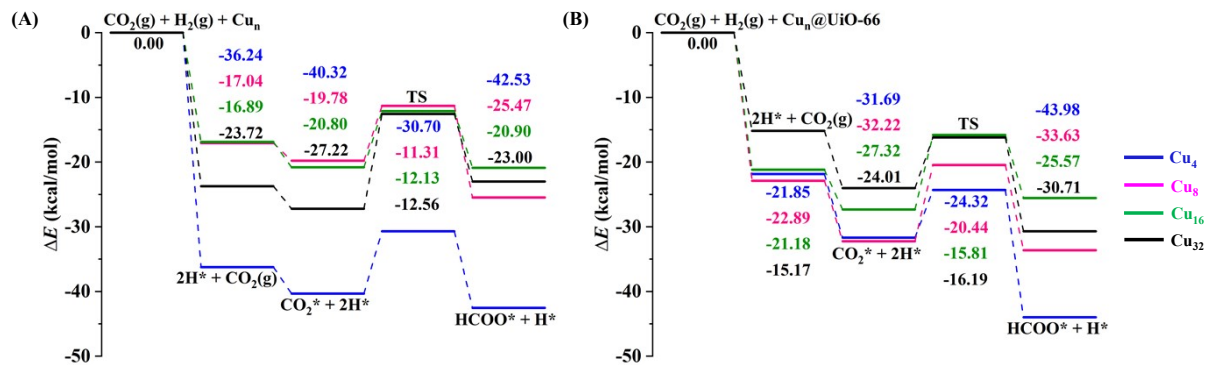


Figure S7. ΔE profiles for CO_2 hydrogenation to HCOO on (A) non-confined and (B) UiO-66 -confined Cu clusters.

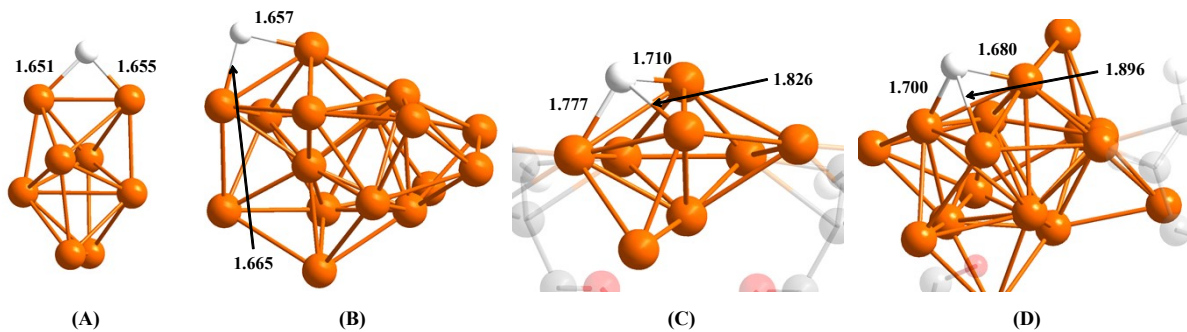


Figure S8. The optimized structures of H^* on Cu_8 , Cu_{16} , $\text{Cu}_8@\text{UiO-66}$ and $\text{Cu}_{16}@\text{UiO-66}$ with key bond distance (\AA), where corresponding adsorption energy of H^* (ΔE_H) is presented in **Table S1**.

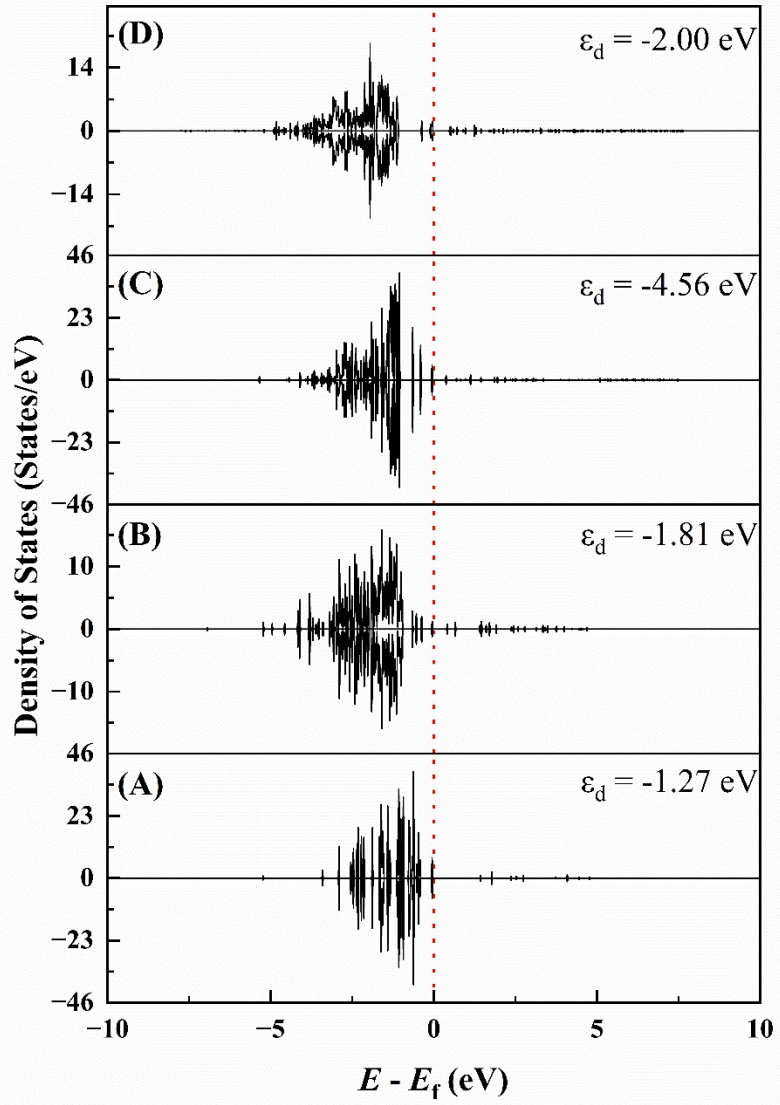


Figure S9. The local density of 3d states of adsorption sites for H^* including corresponding d-band center (ε_d) on (A) Cu_8 , (B) Cu_{16} , (C) $Cu_8@UiO-66$ and (D) $Cu_{16}@UiO-66$, respectively.

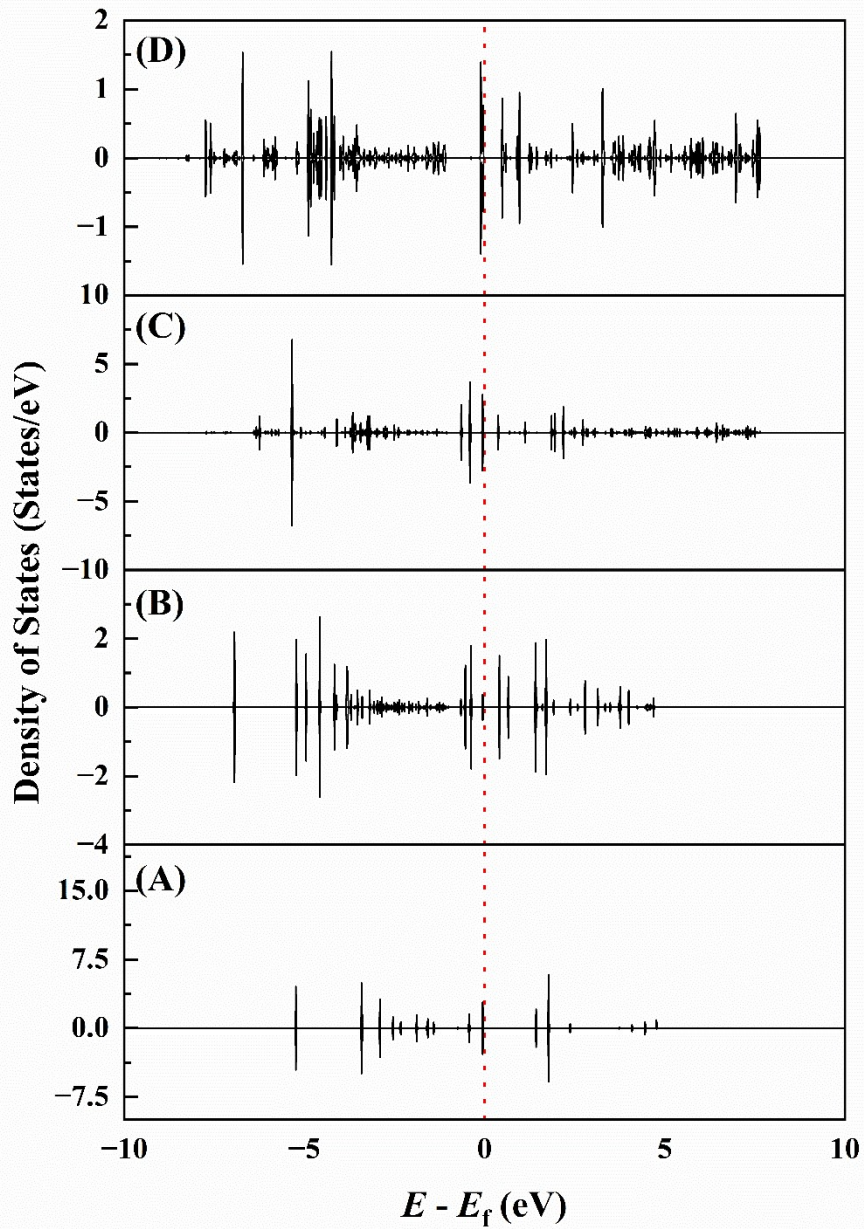


Figure S10. The local density of 4s states of adsorption sites for H* on (A) Cu₈, (B) Cu₁₆, (C) Cu₈@UiO-66 and (D) Cu₁₆@UiO-66, respectively.

S2. Selection of active sites

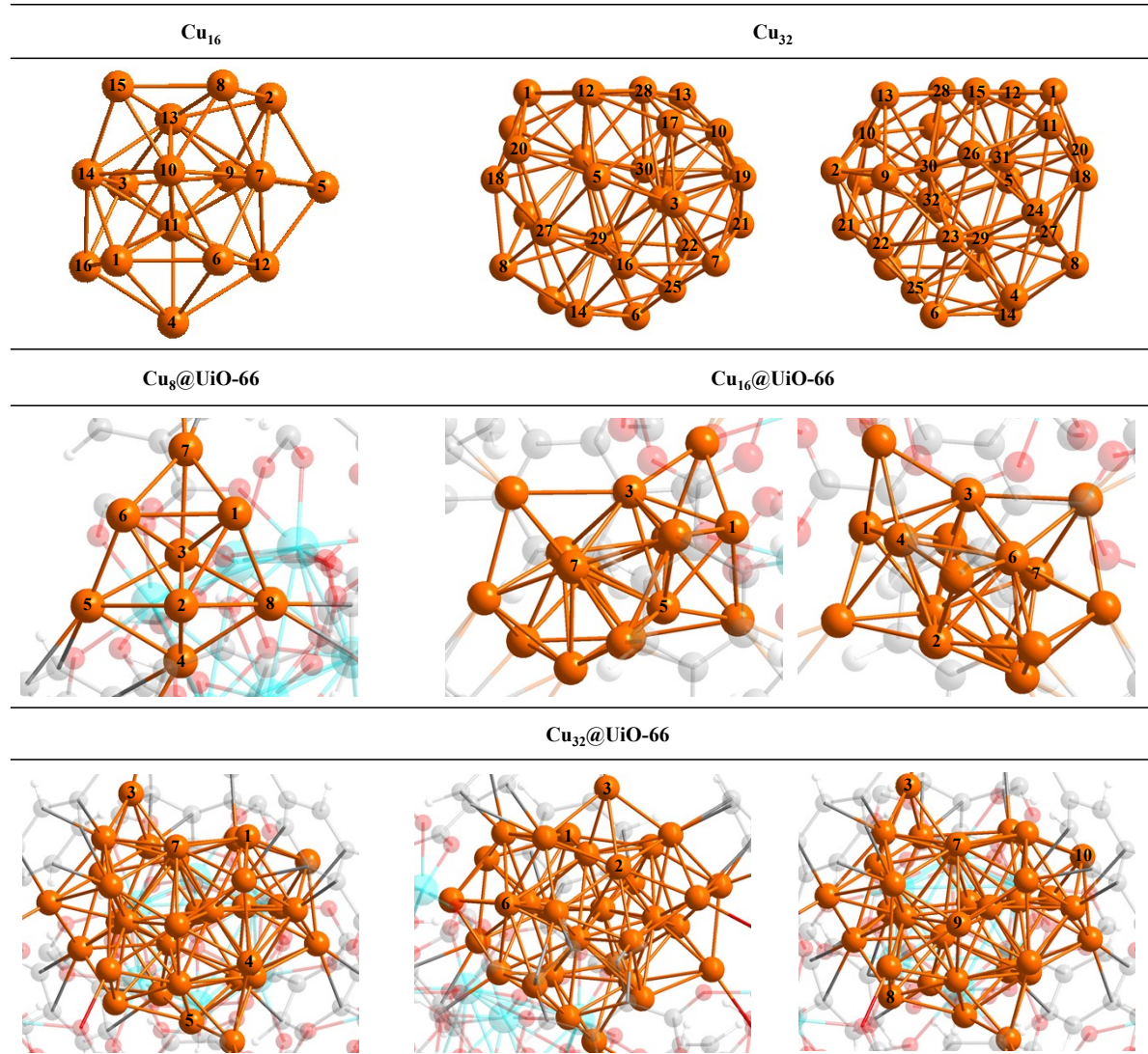


Figure S11. Graphical illustration of Cu sites (CS) assigned for H_2^* on Cu_{16} , Cu_{32} , $\text{Cu}_8@\text{UiO-66}$, $\text{Cu}_{16}@\text{UiO-66}$ and $\text{Cu}_{32}@\text{UiO-66}$, respectively.

In order for an effective C-H interaction, selection of active site for CO_2 hydrogenation is limited to the location of dissociative chemisorption of H_2 reported in our previous study.¹ The initial state of which is H_2^* . We therefore performed calculations of H_2^* on available Cu site (CS) and accordingly computed its ΔE in determining which CS was chosen for H_2 dissociation. Cu_4 and Cu_8 were not examined since their optimal CSs on H_2 dissociation have already been reported by other studies.²⁻⁵ The initial structure of H_2^* on Cu_4 and Cu_8 were

therefore sourced from the literature. On Cu₁₆, all CSs have been assessed (**Figure S11**) and CS8 presents the greatest ΔE of H₂* in contrast to that of other CSs (**Table S2**). On Cu₃₂, CS1 – CS28 were examined as CS29 – CS32 are highly packed by surrounding CSs and located at the core of cluster, resulting in zero activity to H₂ adsorption. As demonstrated in **Table S2**, CS21 is the optimal site for reaction. For Cu₄@UiO-66, only one CS is available to H₂ adsorption as H₂* on the rest of three, which are bonded with UiO-66 as presented in **Figure 1e**, is preferably located at the nearby of window site of UiO-66. For Cu₈@UiO-66 (**Figure S11**), CS6 show the greatest ΔE of H₂* (**Table S2**). CS4 – CS5 and CS7 – CS8, which are in interfacial interactions with UiO-66, as well as CS3 that is highly coordinated by other CSs, show relatively lower adsorption energy in contrast to CS6 (**Table S2**). Therefore, CSs featured with similar characteristics were excluded in the calculations when we came to UiO-66-confined Cu₁₆ and Cu₃₂, where seven and ten CSs were examined, respectively (**Figure S11**). According to **Table S2**, CS2 and CS10 are the results of selection of active site on Cu₁₆@UiO-66 and Cu₃₂@UiO-66.

Table S2. Adsorption energies (ΔE s) of H₂* on Cu sites (CS) of Cu₁₆, Cu₃₂, Cu₈@UiO-66, Cu₁₆@UiO-66 and Cu₃₂@UiO-66, where CS are Cu sites shown in **Figure S11**.

Catalyst ΔE (kcal mol ⁻¹)	Cu ₁₆	Cu ₃₂	Cu ₈ @UiO-66	Cu ₁₆ @UiO-66	Cu ₃₂ @UiO-66
CS1	-4.64	-7.73	-3.05	-2.64	0.04
CS2	-5.99	-10.39	-5.01	-9.09	-0.34
CS3	-1.52	-7.66	-2.70	-5.83	-3.58
CS4	-3.50	-10.05	-3.04	-5.15	-3.69
CS5	-3.94	-7.14	-1.00	-0.97	-4.66
CS6	-4.71	-5.83	-6.63	-3.65	2.69
CS7	-3.95	-8.55	-2.53	-2.11	2.07
CS8	-11.65	-9.12	-1.13		-0.48
CS9	-7.55	-8.34			-3.77
CS10	-6.24	-6.23			-5.21
CS11	-3.56	-7.94			
CS12	-4.79	-9.04			
CS13	-2.16	-9.08			
CS14	-11.38	-6.39			

CS15	-8.39	-4.70
CS16	-2.12	-8.07
CS17		-4.31
CS18		-3.60
CS19		-4.82
CS20		-9.26
CS21		-11.62
CS22		-8.20
CS23		-6.21
CS24		-6.39
CS25		-9.78
CS26		-7.76
CS27		-10.77
CS28		-11.40

S3. Validations of input parameter

For Cu clusters, which are defined as non-periodic systems, are calculated based on $1 \times 1 \times 1$ k-point scheme in precluding spurious interactions from periodic images, thus improving the accuracy on describing their localized electronic states.⁶ By contrast, periodicity is confirmed on UiO-66 composites. Herein, this section aims to search for acceptable k-point grid on sampling their Brillouin zone. Cu₄@UiO-66 was calculated at $1 \times 1 \times 1$, $2 \times 2 \times 2$, $3 \times 3 \times 3$, $4 \times 4 \times 4$, $5 \times 5 \times 5$, $6 \times 6 \times 6$, $7 \times 7 \times 7$, respectively. As demonstrated by **Figure S12**, less-than 0.1 kcal mol⁻¹ derivation between electronic energies at $1 \times 1 \times 1$ and $7 \times 7 \times 7$ is presented, where ΔE_{diff} is the energy difference of various k-point grid using electronic energy computed at $1 \times 1 \times 1$ as benchmark.

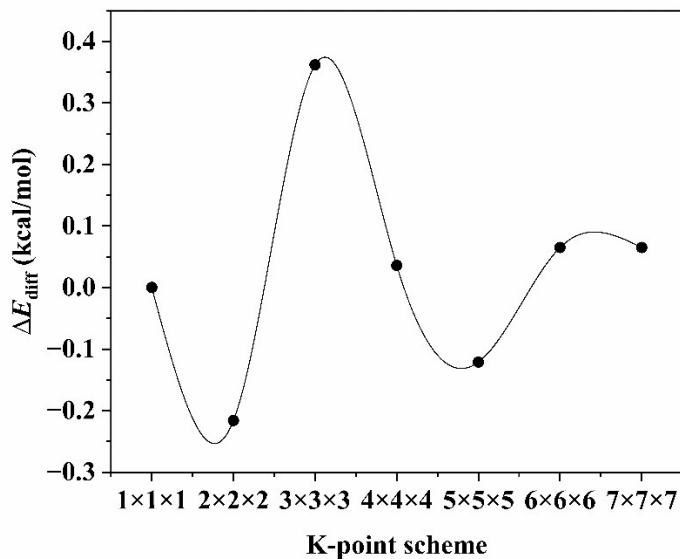


Figure S12. ΔE_{diff} based on $1 \times 1 \times 1$ along various k-point scheme for Cu₄@UiO-66

S4. References

(1) Ye, Z.; Xie, W.; Chen, H.; Kawi, S. How UiO-66 Confinement Tunes Copper Catalytic Activity on H₂ Dissociation? *Mol. Catal.* **2025**, *586*, 115451. <https://doi.org/10.1016/j.mcat.2025.115451>.

(2) Guvelioglu, G. H.; Ma, P.; He, X.; Forrey, R. C.; Cheng, H. Evolution of Small Copper Clusters and Dissociative Chemisorption of Hydrogen. *Phys. Rev. Lett.* **2005**, *94* (2), 026103. <https://doi.org/10.1103/PhysRevLett.94.026103>.

(3) Guvelioglu, G. H.; Ma, P.; He, X.; Forrey, R. C.; Cheng, H. First Principles Studies on the Growth of Small Cu Clusters and the Dissociative Chemisorption of H₂. *Phys. Rev. B* **2006**, *73* (15), 155436. <https://doi.org/10.1103/PhysRevB.73.155436>.

(4) Zhao, S.; Tian, X.; Liu, J.; Ren, Y.; Ren, Y.; Wang, J. Density Functional Study of Molecular Hydrogen Adsorption on Small Gold–Copper Binary Clusters. *J. Clust. Sci.* **2015**, *26* (2), 491–503. <https://doi.org/10.1007/s10876-015-0848-z>.

(5) Lushchikova, O. V.; Tahmasbi, H.; Reijmer, S.; Platte, R.; Meyer, J.; Bakker, J. M. IR Spectroscopic Characterization of H₂ Adsorption on Cationic Cu_n⁺ (*n* = 4–7) Clusters. *J. Phys. Chem. A* **2021**, *125* (14), 2836–2848. <https://doi.org/10.1021/acs.jpca.0c11527>.

(6) Schäfer, T.; Gallo, A.; Irmler, A.; Hummel, F.; Grüneis, A. Surface Science Using Coupled Cluster Theory via Local Wannier Functions and In-RPA-Embedding: The Case of Water on Graphitic Carbon Nitride. *J. Chem. Phys.* **2021**, *155* (24), 244103. <https://doi.org/10.1063/5.0074936>.